Biomedical Applications I

Rule–Based Method for Tumor Recognition in Liver Ultrasonic Images

Vassili A. Kovalev

Computer Center , Belarus Academy of Sciences, Kirova St., 32-A,
246652, Gomel, BELARUS e-mail: goim@nauka.belpak.gomel.by

Abstract. Rule-based method is considered for recognition of arbitrary 64× 64 pixel regions selected in liver ultrasound images. Recognition rules are based on parameters describing spatial distribution of different gradient levels and anisotropy of liver texture. High recognition accuracy has been obtained in case of the same image acquisition conditions.

1 Introduction

There are many approaches for texture characterization based on co-occurrence matrices [1,2], spatial and frequency domain texture features [3], statistical measures, which is not-based on a pre-defined formulation [4], etc. The main problem of the computer analysis and recognition of liver ultrasound texture concerned with great image inhomogeneity [5,6]. Inhomogeneity is due to both anatomical differences between regions of same image and "technical" differences between instruments used and conditions of image acquisition.

The elementary structure balance method [6] based on multidimensional co-occurrence matrices was used at preliminary stage of the work. However, good recognition has been gotten only for the case of one-type regions. It means that only region of interest (ROI) selected and appreciated by specialist in advance can be given in input of a recognition program. So, the following requirements were taken as the initial precondition.

- *A simple choice of the ROI.* The ROI must be as rectangle or square.
- *Arbitrary structure of the ROI.* Any section including liver texture, blood vessel, shadow region, and image edge can be selected in the image analyzed.
- *High automation.* User must not select any regimes and set control parameters.
- *Recognition stability.* It involves in low sensibility to intensity range, image contrast, spatial distortion, and other factors.

Obviously, the requirements listed can be satisfied only using rule-based approach with flexible multi-step scheme of image analysis and recognition.

2 Initial Image Data

Twenty-six liver images of 256×256 pixel size acquired by ultrasonic convex scanner (Fig. 1) were used for parameter selection, recognition rule construction, and testing. The ROI examples of 64×64 pixels are shown in Fig. 2. They present basic types of the liver regions. These examples will be used for illustration of different recognition aspects. Numbers pointed in Fig. 2 over the each ROI will be employed for simplifying references. Seven CT images of 512×512 pixels that present the normal liver were used additionally for estimation of " true " liver texture anisotropy.

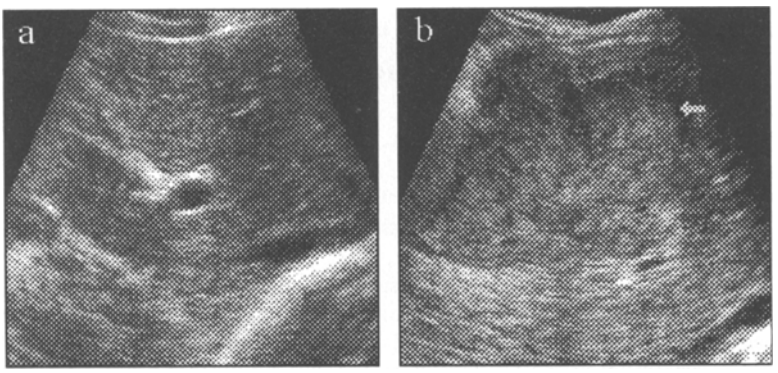

Fig. 1. Example of initial images of normal liver (a) and liver with tumor (b).

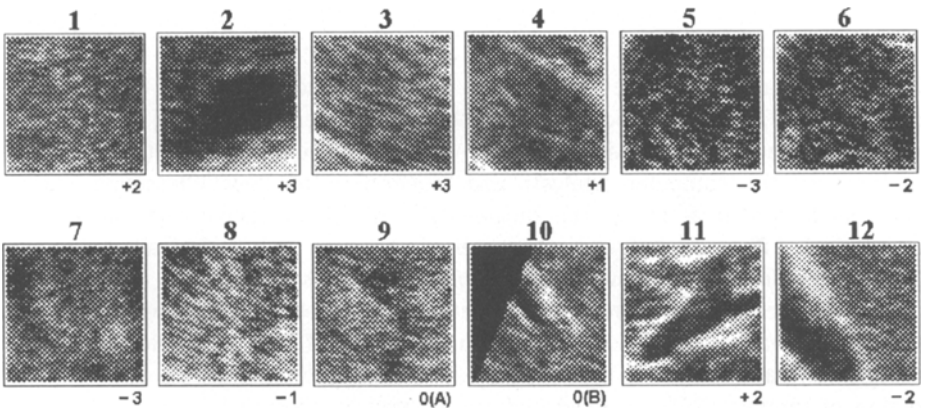

Fig. 2. Example of the liver ROIs: the norm(1-4), the tumor(5-8), and particular cases(9-12).

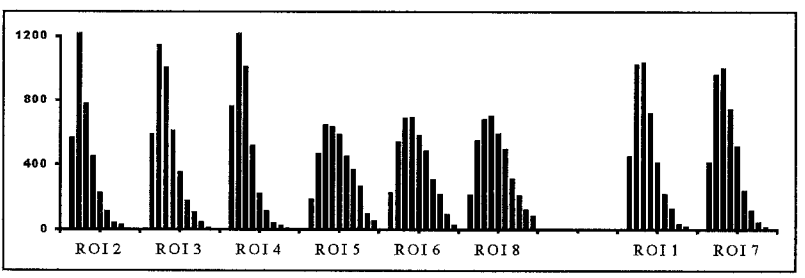

Fig. 3. Gradient histograms for ROIs of Fig. 2: (a) different shape for the norm (ROIs 2-4) and tumor (ROIs 5,6, and 8); (b) similar shape for the norm (ROI 1) and tumor (ROI 7).

3 Method

The parameter (feature) set selection is a key point of the work.

Gradient parameters. The Sobel differential operator with 3×3 mask and root-mean-square magnitude of gradient functions was used for gradient calculation [7]. Investigation of the gradient-based features showed that gradient histograms have as a rule various shapes for the ROI that present the norm and tumor and can be used for recognition (Fig. 3.a). However, in a few isolated cases for typical sections of the

normal liver and tumor histogram shape is similar (Fig. 3.b). The cause is that the histogram shape is not sensitive to global scale-space structure of an image. So, the following procedure was used as a practical manner of the gradient utilizing on account of above mentioned problems.

(a) Dividing of gradient range into four unequal levels (the thresholds used are pointed in the brackets):

code L = 0: "nought" gradient (0-30); code L = 1: small gradient (30-80);

code L = 2: middle gradient (80-300); code L = 3: great gradient (300-800).

(b) Calculation of the quantized gradient image, whose the each pixel is the gradient level code for corresponding pixel of the analyzed ROI.

(c) Segmentation of the gradient image and calculation of every blob area.

(d) Calculation of the "solid" blob area, that is, area without external border pixels and border pixels of holes.

Thus, 8 parameters including area and its solid part as a percentage for each of 4 gradient levels as well as minimum, maximum, and average gradient were selected.

Orientational parameters. By the "orientational parameters" we mean here the quantitative parameters that describe direction and "stretching" degree (anisotropy) of the texture. High spatial image frequency of the liver texture permits to use of the gradient azimuth orientation into 3×3 window as the base of orientational analysis [8]. The orientational histogram was used for the quantitative description of the orientational image structure. It was calculated by the following steps.

(a) The number of intervals (histogram dimension) is chosen, i.e., the number of sectors on which all azimuth range of 0-180 degree are divided (N parameter).

(b) The azimuth orientation of the gradient is calculated for each image pixel with the gradient level code L=2.

(c) The orientational histogram is calculated: $W = (w(1), w(2), \ldots, w(N))$, where w(i) is the number of the image pixels whose the gradient has the azimuth orientation within sector by "i" number. It is convenient to depict the orientational histogram as the circular diagram symmetric about the coordinate center.

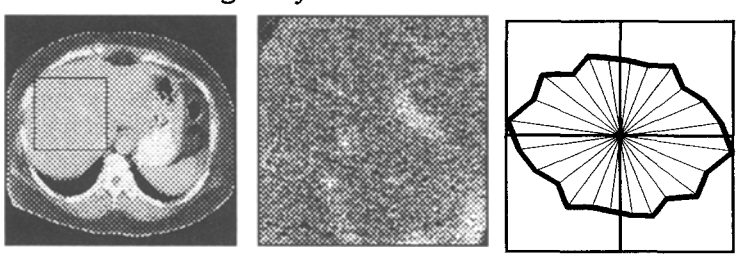

Fig. 4. "True" orientational histogram of liver texture (liver CT image, K_a=1.51).

The anisotropy coefficient $K_a \geq 1.0$ is used as an integral parameter which characterizes the ROI texture anisotropy. It is defined as maximum-to-minimum element ratio of the orientational histogram, i.e. $K_a = Max[w(i)] / Min[w(i)]$. In more details the texture orientational analysis technique discussed in [8]. Typical orientational histogram of normal liver texture are shown in Fig. 4. Investigation of the orientational properties of liver texture showed that the anisotropy decreasing is a symptom of the tumor (Fig. 5). So, the anisotropy coefficient K_a is selected as the

important feature because it characterizes only plane (spatial) properties of the texture and is not sensitive to such transformations as multiplication of the pixel intensity by a constant. The "verticality" coefficient K_V is used as parameter which characterizes the orientation of the ROI structure relatively to image edges. It is determined at N=6 as $K_V = [w(3)+w(4)] / [w(1)+w(6)]$.

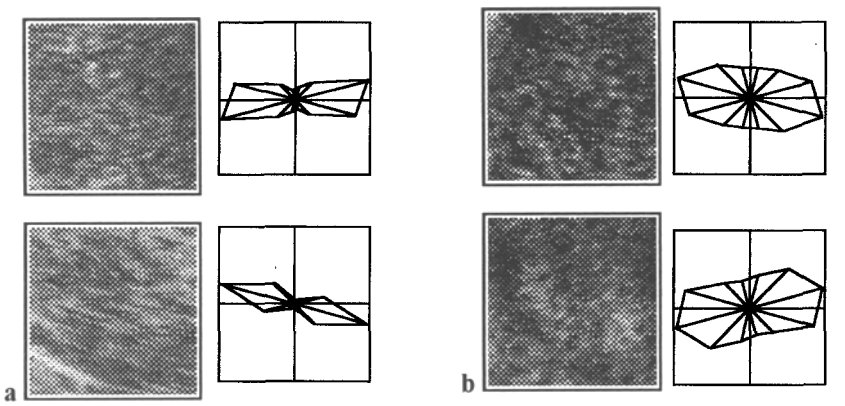

Fig. 5. Orientational histograms for normal and tumor liver regions: (a) normal liver (K_a=8.5 and K_a=15.3); (b) liver with tumor (K_a=2.3 and K_a=2.8).

Diagnostic scale. The ROI recognition result was presented as some diagnostic estimate DS. It indicates that the ROI is related to the norm (DS>0) or to the tumor (DS<0). The confidence of estimate DS is presented in the scale of seven possible levels (colors used for recognition result display are pointed in the brackets).

DS = +3, positive YES (bright green); DS = +2, YES (green);
DS = +1, nonpositive YES (dark green); DS = –3, positive NO (bright red);
DS = –2, NO (red); DS = –1, nonpositive NO (dark red);

The ROI recognition results are ambiguous, i.e., DS = 0 (neutral color) in the cases:

- DS = 0(A). The ROI is some "boundary case" between the norm and tumor;
- DS = 0(B). It is impossible to solve the recognition task due to the poor select of the ROI (great background area, the ROI contains only blood vessel and others);
- DS = 0(C). The selected ROI is not image region.

The ROI diagnostic estimates DS are shown under the each ROI in Fig. 2. All diagnostic estimates are presented except DS=0(C).

Recognition rules. The ROI recognition consists of four stages. 1.Input check of the ROI validity. 2.Setting of initial magnitude for some internal diagnostic estimate IDS. 3.Application of the recognition rules to improving and refinement of internal estimate IDS. 4.Calculation of the final diagnostic estimate DS by the internal estimate IDS and result display.

The input check of the ROI is performed to test an opportunity of recognition task solution, that is, lack of causes for diagnostic estimates as DS=0(B) and DS=0(C). The following recognition rules can be presented as an example.

if (area at L=2 < 15%) *or* (average gradient of ROI < 90) *then* DS=0 (C);
if (area at L=0>10%) *and* (solid at L=0 > 6%) *then* set Edge-Vessel flag;
if (Edge-Vessel flag) *and* ((K_a < 7.0) *or* (K_V > 0.5)) *then* DS=0(B);

Internal variable of recognition algorithm is diagnostic estimate IDS. It shows closeness of the recognition ROI to the norm or tumor in some conditional scale (1.2, 120.0). The anisotropy coefficient K_a is the initial value for IDS. The following rules can be presented as an example of rules used in the third stage.

if (Edge-Vessel flag) *and* ($K_a > 7.0$) *then* increase IDS by 3.0;

if (area at L=3 > 2.5%) *and* (solid at L=3 > 50%) *and* (Edge-Vessel flag) *then* set Vein flag; *if* (Vein flag) *and* ($K_a < 6.8$) *then* increase IDS by 2.5;

if (area at L=1 > 20%) *and* (area at L=3 > 4%) *and* (solid at L=3<10%) *then* increase IDS by 1.5;

The diagnostic estimate DS is determined by the internal estimate IDS at the final fourth stage. The different DS corresponds to the different subintervals of IDS:

IDS:	<3.0	3.0–4.5	4.5–5.4	5.4–6.3	6.3–7.3	7.3–10.0	>10.0
DS:	−3	−2	−1	0(A)	+1	+2	+3

4 Results and conclusions

Sixteen test images of convex ultrasonic scanner acquired by same conditions were used for software checking and recognition quality testing. Eight of them presented the normal liver and eight other -- the liver with tumor. The recognition results were agreed with expert's opinion as a rule (see, for instance, Fig. 2).

The initial images were scanned in raster scan order by 64×64 pixels window with 20 pixel displacement for quantitative estimate of recognition accuracy. So, 100 ROIs were automatically selected in each image. They were differed by 31% pixels as a minimum. General recognition results are presented in Table 1.

Table 1. General recognition results

	ROIs distribution by diagnostic estimate DS								
	−3	−2	−1	0(A)	0(B)	0(C)	+1	+2	+3
Normal liver	0	2	0	4	134	18	26	130	486
Liver with tumor	51	164	66	45	147	21	52	103	151

Normal liver. Nrally, the results with the diagnostic estimate DS<0 (tumor) are qualified as errors in case of normal liver testing (see first row of Table 1). The estimate DS = −2 is taken in two cases (one of them is ROI 12 in Fig. 2). The results DS = −3 and DS = −1 are not taken. So, the recognition errors are 0.25%. The estimate DS=0(A) was taken for four ROIs, that is the ambiguous result are 0.5%. The ROI with number 9 shown in Fig. 2 is a case in point. The main part of rejected ROIs with estimate DS=0(B) and DS=0(C) were obtained from left and right top parts of initial images (see, for example, ROI 10 in Fig. 2).

Liver with tumor. Eight images of liver with tumor are tested by the similar way. Any DS values are possible in the given case because the ROI may include the tumor section, or the normal liver section or some combination of them. Recognition accuracy Ra = 0,1,...6 for every ROI was calculated as the difference between expert's estimate DSe and program estimate DS, i.e., $Ra = |DSe - DS|$. Disagreement magnitude in limits of 1-2 units of confidence scale was qualified as "satisfactory recognition" and more than 2 units -- as a recognition error. The results obtained are shown in Table 2.

Table 2. Recognition accuracy for liver with tumor (632 ROIs).

ROIs	Precise recognition	Satisfactory recognition	Errors
Number of ROIs	517	76	39
Percent	81.8	12.0	6.2

It has been established as a result of special test, the method and software can be applied for tumor recognition in images acquired only by the same scanners and same conditions (ultrasound frequency, spatial resolution, etc.)

Finally, the following recognition results were obtained for all images. 1280 ROIs (without 0(B) and 0(C) cases) were tested. 1163 ROIs (90.9 %) were recognized precisely and 41 ROIs (3.2 %) were recognized with error. Recognition results of 76 other cases (5.9 %) were satisfactory. Prototype software was developed in Pascal for IBM AT compatible computers. The recognition time for 64×64 ROI is about 0.3 second on PC AT 486/66. The following conclusions can be made.

1. The parameters which characterized spatial distribution of different gradient levels and texture anisotropy may be used as features for tumor recognition in liver ultrasound images.

2. Arbitrary liver sections were recognized with high accuracy by the suggested method in case of the same image acquisition conditions.

Acknowledgements - The author wishes to thank MEDISON Co. for providing the initial image data. Special thanks belong to MD S.I.Pimanov for medical verification of the result.

References

1. R.M.Haralick, K.Shanmugam, and I.Dinstein. Textural features for image classification. IEEE Transactions on Systems Man and Cybernetics, SMC-3, No. 6, 1973, pp. 610-621.

2. J.F.Haddon and J.F.Boyce. Co-occurrence matrices for image analysis. Electronics & Communication Engineering Journal, 4, 1993, pp. 71-83.

3. R.Muzzolini, Y.H.Yang, and R.Pierson. Texture characterization using robust statistics. Pattern Recognition, Vol. 27, No. 1, 1994, pp. 119-134.

4. D.Patel and T.J.Stonham. Texture image classification and segmentation using RANK-order clustering. In: Proceedings, 11th Int. Conf. on Pattern Recognition, Vol. 3, The Hague, The Netherlands, 1992, pp. 92-95.

5. J.S. DaPonte and P. Sherman. Classification of ultrasonic image texture by statistical discriminant analysis and neural networks. Computerized Medical Imaging and Graphics, 15(1), 1991, pp.3-9.

6. V.A.Kovalev. Feature extraction and visualization methods based on image class comparison. In: Proceedings, Medical Imaging '94 Int. Symp., Image Processing, M.Loew (ed.), Newport Beach, CA, 1994, pp. 691-701.

7. I.E.Abdou and W.K.Pratt. Quantitative design and evaluation of enhancement/ thresholding edge detectors. IEEE Proc. 67(5), 1979, pp. 753-763.

8. V.A.Kovalev and S.A.Chizhik. On the orientational structure of solid surfaces. Journal of Friction and Wear, Vol. 14, No. 2, Alerton Press, 1993, pp. 45-54.